

# Food & Function

Accepted Manuscript



This article can be cited before page numbers have been issued, to do this please use: R. D. C. L. Lima, R. S. Berg, S. B. Rønning, N. K. Afseth, S. H. H. Knutsen, D. Staerk and S. Wubshet, *Food Funct.*, 2019, DOI: 10.1039/C8FO02450B.



This is an Accepted Manuscript, which has been through the Royal Society of Chemistry peer review process and has been accepted for publication.

Accepted Manuscripts are published online shortly after acceptance, before technical editing, formatting and proof reading. Using this free service, authors can make their results available to the community, in citable form, before we publish the edited article. We will replace this Accepted Manuscript with the edited and formatted Advance Article as soon as it is available.

You can find more information about Accepted Manuscripts in the [author guidelines](#).

Please note that technical editing may introduce minor changes to the text and/or graphics, which may alter content. The journal's standard [Terms & Conditions](#) and the ethical guidelines, outlined in our [author and reviewer resource centre](#), still apply. In no event shall the Royal Society of Chemistry be held responsible for any errors or omissions in this Accepted Manuscript or any consequences arising from the use of any information it contains.

1 **Peptides from chicken processing by-product inhibit DPP-IV and promote cellular** View Article Online  
DOI: 10.1039/C9FO02450B

2 **glucose uptake: potential ingredients for T2D management**

3 Rita de Cássia Lemos Lima,<sup>1</sup> Ragnhild Stenberg Berg,<sup>1</sup> Sissel Beate Rønning,<sup>1</sup> Nils Kristian  
4 Afseth,<sup>1</sup> Svein Halvor Knutsen,<sup>1</sup> Dan Staerk,<sup>2</sup> and Sileshi Gizachew Wubshet<sup>1\*</sup>

5 <sup>1</sup>*NOFIMA AS, Osloveien 1, Ås, Norway*

6 <sup>2</sup>*Department of Drug Design and Pharmacology, University of Copenhagen, Copenhagen,*  
7 *Denmark*

8

9

10

11 \*Corresponding author. Tel.: +47 909 17 126

12 *E-mail address:* sileshi.wubshet@nofima.no (Sileshi G. Wubshet).

13

14

15

16

17

18

19

20

21

**22 Abstract**View Article Online  
DOI: 10.1039/C8FO02450B

23 Inhibition of dipeptidyl peptidase IV (DPP-IV) and stimulation of muscle glucose uptake are  
24 two of the key strategies for management of type-2-diabetes (T2D). In the present study, four  
25 protein hydrolysates generated by enzymatic hydrolysis of chicken by-product, i.e., mechanical  
26 chicken deboning residue, were evaluated for their DPP-IV inhibitory activity as well as their  
27 effect on glucose uptake by skeletal muscle cells. The DPP-IV inhibitory assay was performed  
28 in two concentrations (1000  $\mu\text{g/mL}$  and 10  $\mu\text{g/mL}$ ) for the crude chicken protein hydrolysates.  
29 The hydrolysate with the highest DPP-IV inhibition was selected for preparative-scale  
30 fractionation using size-exclusion chromatography (SEC). The SEC fractions were tested for  
31 DPP-IV inhibitory activity as well as their effect on glucose uptake and metabolic activity of  
32 skeletal muscle cells. The muscle cells were treated with the SEC fractions and glucose uptake  
33 was measured based on luminescence detection of 2-deoxyglucose-6-phosphate (2DG6P). A  
34 fraction with peptides in the lower molecular weight range was shown to promote glucose  
35 uptake and to inhibit DPP-IV. Further chromatographic fractionation followed by inhibition  
36 assaying of the most potent SEC fraction led to isolation of five refined peptide fractions with  
37 more than 80 % DPP-IV inhibition, which were subsequently analyzed with LC-HRMS/MS.  
38 This led to identification of 14 peptides as potential DPP-IV inhibitors from protein  
39 hydrolysates of mechanical chicken deboning residue.

40

41 Keywords: Dipeptidyl peptidase IV, chicken protein hydrolysates, cellular glucose uptake, antidiabetic,  
42 bioactive peptides.

43

44

## 45 1. Introduction

46 Type 2 diabetes (T2D) is a metabolic syndrome characterized by chronic hyperglycemia and is  
47 related to several complications such as nephropathy, retinopathy and neuropathy.<sup>1</sup>  
48 Hyperglycemia is generally provoked by insufficient secretion of insulin by the pancreatic  $\beta$ -  
49 cells or inability of the cells to respond to insulin.<sup>2</sup> About two-thirds of the insulin secretion is  
50 due to the action of the incretin hormones glucagon-like peptide 1 (GLP-1) and glucose-  
51 dependent insulintropic polypeptide (GIP).<sup>3</sup> These hormones are downregulated by dipeptidyl  
52 peptidase IV (DPP-IV), a prolyl peptidase that rapidly cleaves proteins and peptides after a  
53 proline amino acid residue. The half-life of the incretin hormones is short (less than two  
54 minutes), and their degradation by DPP-IV will consequentially have a negative impact on  
55 insulin secretion from pancreatic beta cells. Inhibitors of DPP-IV have therefore become  
56 promising therapeutics for the management of T2D as an alternative to conventional therapies  
57 targeting the decrease of hepatic glucose production (biguanides, i.e. metformin), PPAR- $\gamma$   
58 agonists (i.e. thiazolidinediones), inhibitors of carbohydrases like  $\alpha$ -amylase and  $\alpha$ -glucosidase  
59 (i.e. acarbose, voglibose).<sup>4</sup> Currently, there are few DPP-IV inhibitors in clinical use, such as  
60 sitagliptin, vildagliptin and saxagliptin. Despite efficient hypoglycemic effect, these drugs are  
61 expensive, and their long-term safety remains unestablished.<sup>5</sup> There is, therefore, a need for  
62 alternative sources of DPP-IV inhibitors in the form of functional food or nutraceuticals.

63 An alternative therapeutic approach for management of hyperglycemia is increasing utilization  
64 of glucose by the peripheral tissues and consequently lowering hepatic glucose output. It is well  
65 documented that increasing glucose uptake in muscle cells, in the absence of insulin, can be  
66 achieved through exercise.<sup>6</sup> However, some studies suggest that peptides derived from food  
67 protein can also promote glucose uptake. For example, branched-chain amino acid containing

*Manuscript for Food & Function*

68 dipeptides derived from whey have been shown to promote glucose uptake in both L6 myotubes View Article Online  
DOI: 10.1039/C8FO02450B  
69 and isolated skeletal muscles.<sup>7,8</sup>

70 Over the past decade, a significant number of scientific studies have emphasized the potential  
71 health-promoting effect, including antidiabetic properties, of dietary protein hydrolysates  
72 recovered from a wide range of by-products.<sup>9-13</sup> This has high industrial relevance, since there  
73 is a continued search for feasible applications of food processing by-products that can lead to  
74 increased profits for the producers. Protein hydrolysates from by-products of both plant- and  
75 animal-based food processing have been shown to exhibit antidiabetic activities through  
76 different mechanisms, including  $\alpha$ -glucosidase and DPP-IV inhibition.<sup>14-16</sup> There are a number  
77 of successful developments of bioactive peptides from dairy by-products as food supplements.  
78 However, similar achievements are yet to be accomplished in valorization of meat and poultry  
79 by-products. This is largely due to the high degree of biochemical complexities of meat and  
80 poultry by-products and the resulting peptide mixture generated by, in most cases, non-specific  
81 enzymatic digestion. Therefore, most of the studies on such complex by-products (for example,  
82 poultry by-products) are limited to evaluation of the crude hydrolysates and the observed  
83 activities are seldom ascribed to particular peptides or set of peptides.

84 Among the modern analytical approaches for discovery of bioactive constituents in complex  
85 mixtures is the use of chromatography-coupled bioassays where eluents of a separation are  
86 directed to bio-screenings. Results of the bio-screenings, known as biochromatograms, aligned  
87 with the chemical profiles from the chromatographic detector will provide an excellent tool to  
88 unequivocally pinpoint bioactive constituents or fractions of a complex matrix. This approach,  
89 in combination with mass spectrometry and nuclear magnetic resonance spectroscopy, have  
90 been successfully used to identify bioactive constituents from plant-based crude extracts.<sup>17-20</sup>  
91 In the current study, we have applied such a chromatography-coupled bio-screening strategy to  
92 characterize peptides recovered from protein hydrolysates of a chicken by-product. In addition

*Manuscript for Food & Function*

93 to DPP-IV inhibition, the crude protein hydrolysates and the different peptide fractions were  
94 evaluated for effect on cellular glucose uptake. The sequences of DPP-IV inhibitory peptides  
95 from a chicken by-product as well as their effect on cellular glucose uptake is reported here for  
96 the first time.

View Article Online  
DOI: 10.1039/C8FO02450B

97

98

99

100

101

102

103

104

105

106

107

108

109

110

111

## 112 2. Materials and Methods

View Article Online  
DOI: 10.1039/C8FO02450B

### 113 2.1. Sample material and chemicals

114 Mechanical chicken deboning residue (MCDR) was provided by a Norwegian slaughterhouse  
115 (Nortura, Hærland, Norway). Corolase 2TS was purchased from AB enzymes (Darmstadt,  
116 Germany). DPP-IV from porcine kidney (EC 3.4.14.5) was purchased from Merck (Merck,  
117 Darmstadt, Germany). Protease from *Aspargillus oryzae* (Flavourzyme), insulin, Gly-pro-p-  
118 nitroanilide (GPPN), Tris, diprotin A, HPLC-grade acetonitrile, formic acid, trifluoroacetic acid  
119 (TFA) and molecular weight standards (bovine serum albumin, albumin from chicken egg  
120 white, carbonic anhydrase from bovine erythrocytes, lysozyme, cytochrome C from bovine  
121 heart, aprotinin from bovine lung, insulin chain B oxidized from bovine pancreas, renin  
122 substrate tetradecapeptide porcine, angiotensin II human, bradykinin fragment 1-7, [DAla2]-  
123 leucine enkephalin and Val-Tyr-Val) were purchased from Sigma-Aldrich (St. Louis, MO,  
124 USA). Amphotericin, Dulbecco's Modified Eagle Medium (DMEM), 0.05% trypsin/ EDTA,  
125 fetal bovine serum (FBS) and penicillin/streptomycin solution 10 000 units/mL (P/S) were  
126 purchased from Thermo Fisher Scientific (Waltham, MA, USA). Ultrosor G serum substitute  
127 was purchased from Pall Biosepra (Cergy-Saint-Christophe, France).

### 128 2.2. Production of enzymatic protein hydrolysates

129 The production of hydrolysates was performed according to a previously published protocol.<sup>21</sup>  
130 In short, 500 g of MCDR was homogenized using a food processor and was mixed with 1 L of  
131 water in a Reactor-Ready™ jacketed reaction vessel (Radleys, Saffron Walden, Essex, United  
132 Kingdom). Water circulating through the jacket of the reactor was heated to 50°C and delivered  
133 by a JULABO circulator pump (Julabo, Seelbach, Germany). After slowly mixing the MCDR  
134 until the temperature reaches 50 °C, 7.5 mL of enzyme was added to start the reaction. A total  
135 of four hydrolysates were produced: an 80-min hydrolysate with flavourzyme (RF80), a 240-

136 min hydrolysate with flavourzyme (RF240), a 80-min hydrolysate with corolase (RC80) and a  
137 240-min hydrolysate with corolase (RC240). After the specific hydrolysis time (80 minute or  
138 240 minute), the enzymes were inactivated by heating in a water bath at 95 °C for 15 min.  
139 Contents of the reaction mixture were subsequently centrifuged for 15 min at 4600g and 4 °C  
140 to afford a water-phase supernatant, a fat-phase and solid residue. The water phase was  
141 lyophilized to afford a light yellow-colored powder of protein hydrolysates.

### 142 **2.3. Preparative size exclusion chromatography**

143 Chromatographic separation of the protein hydrolysate RC80 was performed with a Dionex  
144 Ultimate 3000 series instrument (Thermo Scientific, Waltham, MA, USA) equipped with a  
145 quaternary pump, an autosampler, an RS variate wavelength UV-Vis detector, and an  
146 automated fraction collector. Separation was carried out at 25 °C using a Phenomenex BioSpe-  
147 SEC-s2000 column, 300 × 7.8 mm i.d., 5 µm particle size, 145 Å pore size (Phenomenex,  
148 Torrance, CA, USA) and mobile phase consisting of 0.1 M phosphate buffer, pH 6.8. Isocratic  
149 elution was carried out using a flow rate of 4 mL/min for 40 min and monitored at 214 nm. An  
150 injection volume of 1 mL of aqueous solution of RC80 (100 mg/mL) was used and eight  
151 fractions (F1-F8) were collected from 9 to 29 minutes. Collected fractions were lyophilized and  
152 stored at 4 °C before further use. Chromatographic runs were controlled using Chromeleon  
153 software version 7.2 SR4 (Thermo Scientific, Waltham, MA, USA). For the molecular weight  
154 standards an injection solution 2 mg/mL was prepared in water. For each standard, 15 µL was  
155 injected and separation was performed with the same condition as for the samples above.

### 156 **2.4. Preparative-scale reversed-phase chromatography**

157 Orthogonal chromatographic separation of fraction F5 was performed using a Dionex Ultimate  
158 3000 series instrument (Thermo Scientific, Waltham, MA, USA) equipped with a quaternary  
159 pump, an autosampler, an RS variate wavelength UV-Vis detector, and an automated fraction



160 collector. 1 mL of aqueous solution of fraction F5 (100 mg/mL) was separated at 25 °C using  
161 a Thermo Betasil C<sub>18</sub> column, 250 × 10 mm i.d., 10 µm particle size (Thermo Scientific,  
162 Waltham, MS, USA). Mobile phase consisted of water (solvent A) and acetonitrile (solvent B),  
163 both acidified with 0.05% of TFA, and the flow rate was kept at 4 mL/min. A gradient elution  
164 was carried out as follows: 0 min, 0% B; 10 min, 0% B; 45 min, 40% B; 50 min, 100% B; 60  
165 min, 100% B. The separation was monitored at 214 nm, and 18 fractions were collected from  
166 13 to 40 minutes. Fractions from a single separation were subsequently lyophilized and used  
167 for DPP-IV inhibition. Subsequently, four similar separations were performed and collected  
168 fractions were pooled and used for LC-MS/MS analysis. Chromatographic separation was  
169 controlled using Chromeleon software version 7.2 SR4 (Thermo Scientific, Waltham, MA,  
170 USA).

## 171 2.5. DPP-IV inhibition assays

### 172 2.5.1. Screening of crude protein hydrolysates and fractions

173 The crude hydrolysates were assayed using final concentrations 10 µg/mL or 1000 µg/mL  
174 whereas the SEC fractions were assayed using a final concentration of 1000 µg/mL. Test  
175 samples of the lyophilized reversed phase fractions were prepared by directly dissolving the  
176 lyophilized fractions in 20 µL of assay buffer. The DPP-IV inhibition assay was performed  
177 according to Al-Masri et al. (2009) with slight modifications.<sup>22</sup> In short, experiments were  
178 performed in triplicate in 96-well microplates with a final volume of 100 µL. 20 µL test sample,  
179 22.5 µL of Tris-HCl buffer pH 7.5, and 7.5 µL of DPP-IV enzyme solution in Tris-HCl buffer  
180 pH 7.5 (0.05 U/mL final concentration) were added to each well. The mixture was incubated  
181 for 10 minutes at 37 °C, whereafter 50 µL of GPPN (0.2 mM in Tris-HCl, pH 7.5) was added  
182 to the mixture. The absorbance was subsequently measured at 405 nm every 1 min for 30 min,  
183 using a Synergy H1 hybrid multi-mode microplate reader (Biotek, Winooski, VT, USA).

184 Diprotin A was used as a positive control. The percentage of DPP-IV inhibition was calculated  
 185 using the following formula:

$$186 \quad \% \text{ Inhibition} = 1 - \left( \frac{\text{Slope}_{\text{sample}}}{\text{Slope}_{\text{control}}} \right) \times 100$$

### 187 2.5.2. Determination of DPP-IV IC<sub>50</sub> values for RC80 and fraction F5

188 The DPP-IV IC<sub>50</sub> values of RC80 and the active fraction F5 were determined using the standard  
 189 methods described in Section 2.5.1. The percentage of inhibition of DPP-IV was calculated as  
 190 mean ± standard deviation in Microsoft Excel using the above-described formula. The results  
 191 were thereafter exported and used to assess the dose-response curves and IC<sub>50</sub> values in  
 192 GraphPad Prism, version 7.04 software (La Jolla, CA, USA). Data were fitted into the equation:

$$193 \quad f(x) = \min + \frac{\max - \min}{1 + \left( \frac{x}{IC_{50}} \right)^{\text{slope}}}$$

194 where min is the background, max-min is the y-range, x is the concentration and slope is the  
 195 Hill slope.

## 196 2.6. In vitro primary skeletal muscle cells

### 197 2.6.1. Cell seeding and treatment

198 Bovine primary skeletal muscle satellite cells were isolated as previously described.<sup>23</sup> Animals  
 199 of the same age (young animals), gender (bulls) and breed (Norwegian Red) were used for the  
 200 muscle cell isolation. In brief, small muscle pieces of ~ 1 g were digested for 1h with 70 rpm  
 201 shaking in 10 mL DMEM with 0.72 mg/ml collagenase, 10 000 units/mL P/S and 250 µg/mL  
 202 amphotericin B at 37°C. The muscle cells were subsequently dissociated from surrounding  
 203 tissue by three cycle treatments (of 25 min each) with 0.05% trypsin/EDTA. 10% FBS were

204 added after each treatment to inactivate trypsin and harvested cells were pooled. For removal  
205 of fast-adhering fibroblasts from the primary muscle cell cultures, the cells were placed in un-  
206 coated cell flasks for 1 h at 37 °C which allowed the fibroblasts to adhere to the plastic. The  
207 non-adhering primary muscle cells were then collected in low glucose DMEM GlutaMAX™  
208 containing 2% FBS, 2% Ultrosor G, P/S (10 000 units/mL) and amphotericin B (250 µg/mL),  
209 seeded out (3000 cells/well) in to a 96 well plate and were grown for four days until 70-80 %  
210 confluence. Subsequently, the cells were placed in differentiation medium (i.e., DMEM  
211 containing 2% FBS, P/S (10 000 units/mL) and amphotericin B (250 µg/mL) and 25 pmol  
212 insulin) for three days to induce myogenesis. The differentiated primary bovine muscle cells  
213 were then used to measure glucose uptake and cell viability (ATP production).

#### 214 2.6.2. Cell glucose uptake and metabolic activity measurements

215 Both glucose uptake and metabolic activity (viability) measurements were performed in  
216 triplicates. One day prior to treatment with the hydrolysate fractions, the differentiated primary  
217 bovine muscle cells were starved with serum free medium for 24 hours. For the glucose uptake  
218 study, the cells were treated with 100 µL of 1 mg/mL solution of the eight SEC fractions (F1-  
219 F8) for 1 hr at 37 °C and with 5% CO<sub>2</sub>. Glucose uptake, after the treatment, was measured based  
220 on luminescence detection of 2-deoxyglucose-6-phosphate (2DG6P). The measurements were  
221 performed using a Glucose Uptake-Glo™ Assay kit (Cat# J1341; Promega, Madison, WI, US).  
222 Incubation with insulin (1 mM) was used as a positive control and percentage glucose uptake  
223 was calculated relative to untreated cultures (100 % glucose uptake). As a negative control,  
224 glucose uptake was calculated for cells without addition of 2-deoxyglucose (-2DG) and with  
225 addition of stop buffer prior to 2DG (stopped). Effect of the eight SEC fractions (at a final  
226 concentration of 500 µg/mL) on metabolic activity of the cells in the culture was measured  
227 based on quantification of the ATP present. The differentiated cells were treated with 100 µL

228 of 1 mg/mL solution of the eight SEC fractions (F1-F8) for 1 hr at 37 °C and with 5% CO<sub>2</sub> and  
229 relative quantification of ATP production was determined using a Promega CellTiter-Glo®  
230 luminescent cell viability assay kit (Cat# G9241; Promega, Madison, WI, US). Percentage ATP  
231 production for the cultures treated with the SEC fractions was calculated relative to untreated  
232 cultures (100 % ATP production). Luminescence was measured using a Synergi H1 hybrid  
233 multi-mode reader (BioTek Instruments, Inc., Winooski, VT, USA)

## 234 2.7. HPLC-HRMS analysis

235 An injection solution of each sample was prepared by dissolving the freeze-dried fraction in 50  
236 % methanol. High-performance liquid chromatography-high-resolution mass spectrometry  
237 (HPLC-HRMS) analyses of fractions F5-4, F5-5, F5-13, F5-14, and F5-16 were performed on  
238 a Agilent 1260 chromatograph consisting of a G1322A degasser, a G1311A quaternary pump,  
239 a G1316A thermostatted column compartment, and a G1315A photodiode-array detector (Santa  
240 Clara, CA, USA) hyphenated with a Bruker micrOTOF-Q II mass spectrometer equipped with  
241 an electrospray ionization (ESI) interface and controlled by Bruker Hystar software version 3.2  
242 (Bruker Daltonik, Bremen, Germany). Separation of freeze-dried samples re-dissolved in 50 %  
243 methanol were performed on a reversed-phase Phenomenex Luna® Omega Polar C<sub>18</sub> column,  
244 250 × 4.6 mm, 5 mm particles, 100 Å pore size (Phenomenex, Torrance, CA, USA) using an  
245 injection volume of 10 µL. The flow rate was maintained at 0.5 mL/min, using the following  
246 gradient elution profile of mobile phase A (water/acetonitrile 95:5 v/v) and mobile phase B  
247 (water/acetonitrile, 5:95 v/v), both acidified with 0.1% formic acid: 0 min, 0% B; 5 min, 0% B;  
248 25 min, 100% B; 35 min, 100% B; 37 min, 0% B. Automated MS/MS spectra were acquired in  
249 positive ion mode, using a drying temperature of 200 °C, a nebulizer pressure of 2.0 bar, and a  
250 drying gas flow of 7 L/min. For smaller molecular weight peptides (less than 500 Dalton)  
251 identification was performed manually by studying the fragmentation patterns. For peptides of  
252 8 amino acid residues or more, database-assisted identification was performed using MaxQuant

*Manuscript for Food & Function*

253 software version 1.6.2.3.<sup>24</sup> Raw LC-HRMS/MS data was searched against unspecific digest of View Article Online  
DOI: 10.1039/C8FO02450B

254 *Gallus gallus* (Chicken) proteins (UniProtKB database).

255

256

257

258

259

260

261

262

263

264

265

266

267

268

269

270

271

### 272 3. Results and discussion

273 Four crude protein hydrolysates produced from mechanical chicken deboning residues  
274 (hydrolyzed for 80 or 240 minutes) using flavourzyme (RF80 and RF240) and corolase (RC80  
275 and RC240) as catalytic proteases were assessed for their DPP-IV inhibition. The hydrolysate  
276 with the highest activity was fractionated using SEC, and these fractions were assessed for their  
277 DPP-IV inhibitory activity as well as their effect on glucose uptake. This led to isolation of the  
278 most bioactive fraction F5. Following further reversed-phase chromatographic fractionation of  
279 F5, DPP-IV inhibition assaying, and LC-HRMS/MS analysis, the most promising  
280 hypoglycemic peptides were identified. A summary of the work flow is presented in **Figure 1**.

#### 281 3.1. DPP-IV inhibition of the chicken protein hydrolysates

282 A preliminary assessment for DPP-IV inhibition, at two different concentrations showed that  
283 the crude hydrolysates had 45% to 60% inhibition at 1 mg/mL (**Table 1**). Recent studies have  
284 shown that by-products from macroalgae, fish, whey protein, and chicken egg proteins have  
285 potential antidiabetic effects due to DPP-IV inhibition.<sup>15, 25</sup> However, to the best of our  
286 knowledge, this is the first report of chicken byproduct hydrolysates as source of DPP-IV  
287 inhibitors. One of the trends observed from the preliminary screening was a decrease in DPP-  
288 IV inhibition with an increase of the hydrolysis time from 80 to 240 minutes. This could be a  
289 result of breakdown of the bioactive peptides into single amino acids. The most active  
290 hydrolysate (RC80) from the screening was found to have an IC<sub>50</sub> value of 0.919 mg/mL  
291 (**Figure S1**). This IC<sub>50</sub> value is comparable to previously reported DPP-IV inhibition by protein  
292 hydrolysates from different sources.<sup>26,27</sup> Thus, the mechanical chicken deboning residue  
293 hydrolyzed with corolase for 80 minutes (RC80) was chosen for an in-depth analysis and  
294 identification of its bioactive constituents.

### 295 3.2. SEC-coupled DPP-IV inhibition

View Article Online  
DOI: 10.1039/C8FO02450B

296 Raw protein hydrolysates contain molecules ranging from unhydrolyzed large proteins to  
297 simple amino acids. Therefore, a targeted study of bioactive constituents usually requires a  
298 fractionation or a filtration procedure. In the current study, the most active protein hydrolysate  
299 (RC80) was subjected to SEC fractionation, where eight fractions (F1-F8) were automatically  
300 collected (**Figure 2A**). The overall chromatogram of RC80 showed abundance of constituents  
301 in lower molecular weight range (retention time below 19 min). After measuring the DPP-IV  
302 inhibition for the eight fractions, the bioactivity profile (**Figure 2B**) was plotted under and was  
303 correlated to chromatographic trace (**Figure 2A**). This provided a tool to identify and guide a  
304 targeted isolation the promising bioactive peptide fraction. The most active fraction (F5) was  
305 eluted from 19-21 min and showed 54 % inhibition of DPP-IV (**Figure 2B**). This promising  
306 fraction (F5) was therefore subjected to dose-dependent DPP-IV assessment and was found to  
307 have an  $IC_{50}$  of 0.155 mg/mL. This showed that this fraction possesses approximately six-fold  
308 higher DPP-IV inhibitory activity than that of the raw protein hydrolysate (RC80;  $IC_{50} = 0.919$   
309 mg/mL). The increased DPP-IV inhibition of fraction F5 is a result of the targeted fractionation  
310 of the most bioactive peptides assisted by the bioactivity profile (**Figure 2B**).

### 311 3.3. Effect of peptide fractions on cellular glucose uptake and metabolically 312 active cells

313 The eight SEC fractions (F1-F8) were studied for their effect on glucose uptake by skeletal  
314 muscle cells. The results showed that three of the eight fractions (F-5, F-6 and F-7) induced  
315 cellular glucose uptake (**Figure 3A**). Particularly, fraction F5 resulted in increased glucose  
316 uptake by 41.6 % at a concentration of 1 mg/mL. Recent studies have reported positive effects  
317 of peptides from soybeans and flaxseeds protein hydrolysates on glucose uptake.<sup>28</sup> Moreover,  
318 it has been reported that an improved glucose uptake effect might be related to specific low

319 molecular weight peptides (between 300-400 kDa).<sup>28,29</sup> To the best of our knowledge, this is View Article Online  
DOI: 10.1039/C8FO02450B

320 the first study reporting the positive effect of peptides from chicken hydrolysates on glucose

321 uptake. In addition to the glucose uptake, the fractions F1-F8 were tested for the effect on

322 metabolic activity of the cells by measuring the ATP present in the cell cultures. In particular

323 fraction F5 decreased ATP production in the cell culture (**Figure 3B**), but also fractions F3, F4

324 and F6 seems to decrease ATP production - albeit to a lower extent. One possible explanation

325 to this result might be activation of AMP-activated protein kinase (AMPK). AMPK is suggested

326 to be one of the targets of major antidiabetic drugs, such as thiazolidinediones and the

327 biguanides, as well as insulin sensitizing adipokines, although the mechanism seems to be

328 indirect.<sup>30,31</sup> Several studies suggest that AMPK plays an important role during muscle glucose

329 uptake during pharmacological stimuli which is consistent with the observed lowest ATP

330 production for cells stimulated with F5 (a fraction correlated with highest glucose uptake).<sup>32</sup>

331 AMPK function as a sensor of intracellular energy, and pharmacological activation of AMPK

332 has been shown to promote glucose transport.<sup>33</sup> At the same time, AMPK is activated by

333 increased cellular level of AMP:ATP and ADP:ATP ratios, which could explain the reduced

334 ATP levels observed in the cell culture stimulated with F5.<sup>32,34</sup> The high complexity of the

335 mechanisms and receptors involved in cellular glucose uptake, in particular the AMPK pathway

336 upon peptide treatment, requires further investigations in order to establish the most probable

337 pathways responsible for the activity of the tested fractions.

#### 338 **3.4. Reversed-phase chromatography-coupled DPP-IV inhibition**

339 Despite preliminary SEC fractionation, the protein hydrolysate fractions are still typically

340 associated with a high degree of complexity. One of the successful analytical approaches to

341 resolve constituents of complex biological matrices is sequential orthogonal chromatographic

342 separations.<sup>35</sup> In this study, a reversed-phase chromatography separation, orthogonal to the

343 preceding SEC fractionation, was performed on the bioactive fraction F5 and a total of 18



344 reversed-phase fractions were automatically collected from 13 to 40 minutes (**Figure 4A**).  
345 These fractions were subsequently evaluated for their DPP-IV inhibitory activity. The  
346 bioactivity of the different fractions was plotted against the retention time leading to a semi-  
347 high-resolution DPP-IV inhibition profiling (**Figure 4B**). The majority of the fractions were  
348 shown to have moderate to high activity, and fractions F5-4, F5-5, F5-13, F5-14 and F5-16,  
349 showed DPP-IV inhibitory activity above 80% (highlighted in **Figure 4A**). The highest  
350 activities were observed for both early eluting peptides (F5-4 and F5-5) as well as the three late  
351 eluting peptides fractions (F5-13, F5-14 and F5-16). This is in contrast to a previous study,  
352 which has proposed a link between retention time of peptides in a reversed-phase column and  
353 DPP-IV inhibitory activity.<sup>15</sup> The five most active fractions were subjected to LC-HRMS/MS  
354 analyses for identification of bioactive peptides.

### 355 3.5. Identification of bioactive peptides

356 The base peak chromatograms of fractions F5-4, F5-5, F5-13, F5-14 and F5-16 are presented  
357 in **Figure 5**. The complete list of the 19 major constituents from these five most bioactive  
358 fractions with retention time, MS/MS results and identified peptides is presented in Table 2. In  
359 addition, all the MS and MS/MS spectra are provided in supplementary information (**Figure**  
360 **S2-S19**). Of the 19 major constituents, a very high degree of complexity in the MS/MS spectra  
361 hampered identification of peaks 2, 11, 13, 16 and 18. These complexities are largely due to  
362 parent and daughter ions of co-eluting multiple constituent.

363 In fraction F5-4, MS spectra of the peptide eluted as peak 1 showed a molecular ion peak of  
364 233.1499 [M+H]<sup>+</sup> which was assigned to the formula C<sub>10</sub>H<sub>21</sub>N<sub>2</sub>O<sub>4</sub><sup>+</sup> ( $\Delta = 1.4$  ppm). After  
365 studying the diagnostic fragment ions in the MS/MS spectrum, the peptide eluted as peak 1 was  
366 identified as thronyl-leucine (TL).<sup>36</sup> Similarly, after comparing the MS fragment ions with  
367 reference values, the material eluted as peak 3 (221.0937 [M+H]<sup>+</sup>, C<sub>11</sub>H<sub>13</sub>N<sub>2</sub>O<sub>3</sub><sup>+</sup>,  $\Delta = 7.4$  ppm)

368 was tentatively assigned as 5-hydroxytryptophan.<sup>37</sup> The presence of this compound was  
369 unexpected and is most likely an oxidation product of the naturally occurring tryptophan.  
370 Oxidation of amino acids and peptides during enzymatic hydrolysis is a common  
371 phenomenon.<sup>37</sup> The molecular ion of the peptide eluted as peak 4 was assigned to  $C_{13}H_{17}N_2O_5^+$   
372 ( $\Delta = 1.3$  ppm). This molecular formula and observed MS/MS fragment ion peaks were  
373 consistent with aspartyl-phenylalanine (DF).<sup>38</sup>

374 With retention time and MS/MS spectra similar to the peptide eluted as peak 1 of fraction F5-  
375 4, the peptide eluted as peak 5 from fraction F5-5 was also identified as TL. After studying the  
376 major fragment ions, the peptide eluted as peak 6 (203.1390  $[M+H]^+$  ( $C_9H_{19}N_2O_3^+$ ,  $\Delta$  4.9 ppm)  
377 was identified as leucyl-alanine (LA).<sup>39</sup> This peptide has previously been reported to have DPP-  
378 IV inhibitory activity with an  $IC_{50}$  value of  $0.091 \pm 0.006$  mM.<sup>40</sup> The fragmentation of the  
379 peptide eluted as peak 7 (461.2242  $[M+H]^+$ ,  $C_{19}H_{33}N_4O_9^+$ ,  $\Delta = 1.2$  ppm) was consistent with  
380 the tripeptide leucyl-alanyl-aspartic acid (LAD) (**Figure 6A**). Similarly, after assigning  
381 characteristic *a*, *b* and *y* fragment ions, the peptide eluted as peak 8 (476.2308  $[M+H]^+$ ,  
382  $C_{10}H_{21}N_2O_4^+$ ,  $\Delta = 1.4$  ppm)) was identified as valine-glutamic acid-valine-aspartic acid  
383 (VEVD) (**Figure 6B**). The MS/MS spectra of peak 7 and 8 together with the complete fragment  
384 ion assignments are presented in **Figure 6**.

385 The peptides eluted as the two major peaks of fraction F5-13, peak 9 and 10, were identified as  
386 isobaric peptides with molecular formula of  $C_{12}H_{24}N_2O_3$ . The fragmentation pattern of both  
387 peaks was similar and consistent with a dipeptide containing two leucine or isoleucine residues.  
388 Therefore, the two peaks were tentatively assigned as structural isomers of leucyl-leucine (LL).  
389 Both LL and IL have previously been identified from *in vitro* gastrointestinal digestion products  
390 of Brewers' spent grain protein hydrolysates as DPP-IV inhibitor.<sup>41</sup>

*Manuscript for Food & Function*

391 The peptide eluted as peak 12 from fraction F5-14, was identified as a nonapeptide, i.e.  
392 ETGKGEDGE, using the MaxQuant algorithm. The peptide eluted as peak 14 had similar  
393 retention time, molecular ion peak and MS fragmentation pattern as the peptide eluted as peak  
394 10 and is therefore tentatively identified as LL. The molecular ion peak as well as fragmentation  
395 ions observed for the peptide eluted as peak 15 (279.1710 [M+H]<sup>+</sup>, C<sub>15</sub>H<sub>23</sub>N<sub>2</sub>O<sub>3</sub><sup>+</sup>, Δ = 2.6 ppm)  
396 were consistent with phenylalanyl-leucine (FL). This di-peptide has previously been reported  
397 as competitive inhibitor of DPP-IV with an IC<sub>50</sub> value of 399.58 ± 10.81 μM.<sup>42</sup>

398 The peptide eluted as peak 17 from fraction F5-16 was identified as an octapeptide  
399 LFFSMLLML using MaxQuant. The peptide eluted as peak 19 (279.1706 [M+H]<sup>+</sup>,  
400 C<sub>15</sub>H<sub>23</sub>N<sub>2</sub>O<sub>3</sub><sup>+</sup>, Δ = 0.9 ppm) was observed to have the same molecular ion peak and elute at the  
401 same retention time as peak 15. However, after a careful analysis of diagnostic fragment ions,  
402 the peptide eluted as peak 19 was identified as leucyl-phenylalanine (LF), a structural isomer  
403 of the di-peptide eluted as peak 15. One of the characteristic differences observed between the  
404 MS/MS spectra of the peptides eluted peak 15 and 19 was the relative intensities of *m/z* 86 and  
405 120. The base peak for LF, *m/z* 86, appear to be lower in FL, while the base peak for FL, *m/z*  
406 120, is lower in LF. Similar diagnostic analysis of fragment ions has previously been reported  
407 as a strategy to differentiate the two structural isomers.<sup>43</sup>

408 The majority of peptides identified from the DPP-IV-inhibiting fractions were dipeptides.  
409 Several studies have suggested that dipeptides derived from dietary protein can act as potent  
410 inhibitors of DPP-IV.<sup>26</sup> Another interesting observation was related to terminal leucine or  
411 isoleucine residue.<sup>44</sup> All the five fractions with the highest DPP-IV activity was found to contain  
412 at least one peptide with leucine or isoleucine as a terminal residue. This is consistent with a  
413 previous *in silico* study which showed a general trend of high DPP-IV inhibition for peptides  
414 containing hydrophobic or aromatic amino acids at the N-terminal.<sup>45</sup> DPP-IV inhibitory activity

415 of peptides containing amino acids, such as leucine or isoleucine at the N-terminal, is likely a  
416 result of interactions with the hydrophobic motifs of the enzyme's catalytic pockets.<sup>46</sup>

#### 417 **4. Conclusion**

418 In the present study, peptides derived from mechanical chicken deboning residues were shown  
419 to have potential antidiabetic activity. A low molecular weight peptide fraction (F5) from SEC  
420 separation of the chicken by-product protein hydrolysate was found to inhibit DPP-IV *in vitro*  
421 and promote cellular glucose uptake *ex vivo*. A series of chromatographic fractionations and  
422 mass spectrometric analyses led to identification of the peptides constituting the DPP-IV  
423 inhibiting fractions. Common to all fractions with highest DPP-IV inhibition activity was the  
424 presence of one or more peptides with an N-terminal leucine or isoleucine residue. These results  
425 suggest that these peptide fractions prepared from mechanical chicken deboning residues can  
426 potentially serve as ingredients of multi-functional foods with dual effects of DPP-IV inhibition  
427 and enhancement of cellular glucose uptake.

#### 428 **Conflicts of interest**

429 There are no conflicts of interest to declare.

#### 430 **Acknowledgment**

431 The Norwegian Research Council is greatly acknowledged for the financial support through  
432 projects no. 261849/F20 and 262300/F40.

433

434

435

436

437

438 **References**View Article Online  
DOI: 10.1039/C8FO02450B

- 439 1. G. Alberti, P. Zimmet, J. Shaw, Z. Bloomgarden, F. Kaufman and M. Silink, Type  
440 2 diabetes in the young: the evolving epidemic, *Diabetes Care*, 2004, **27**, 1798-  
441 1811.
- 442 2. International Diabetes Federation, *IDF Diabetes Atlas* 8th ed., International  
443 Diabetes Federation, Brussels, Belgium 2017.
- 444 3. B. Richter, E. Bandeira-Echtler, K. Bergerhoff and C. L. Lerch, Dipeptidyl  
445 peptidase-4 (DPP-4) inhibitors for type 2 diabetes mellitus, *Cochrane Database*  
446 *Syst. Rev.*, 2008, **2**, 1-154.
- 447 4. D. Moller, New drug targets for type 2 diabetes and the metabolic syndrome,  
448 *Nature*, 2001, **414**, 821-827.
- 449 5. D. M. Nathan, J. B. Buse, M. B. Davidson, E. Ferrannini, R. R. Holman, R.  
450 Sherwin and B. Zinman, Medical management of hyperglycemia in type 2  
451 diabetes: a consensus algorithm for the initiation and adjustment of therapy,  
452 *Diabetes Care*, 2009, **32**, 193-203.

- 453 6. J. L. Ivy and J.O. Holloszy, Persistent increase in glucose uptake by rat skeletal  
454 muscle following exercise, *Am. J. of Physiol.*, 1981, **24**, C200-203.
- 455 7. M. Morifuji, J. Koga, K. Kawanaka and M. Higuchi, Branched-chain amino acid-  
456 containing dipeptides, identified from whey protein hydrolysates, stimulate  
457 glucose uptake rate in L6 myotubes and isolated skeletal muscles, *J. Nutr. Sci.*  
458 *Vitaminol.*, 2009, **55**, 81-86.
- 459 8. M. Soga, A. Ohashi, M. Taniguchi, T. Matsui and T. Tsuda, The di-peptide Trp-  
460 His activates AMP-activated protein kinase and enhances glucose uptake  
461 independently of insulin in L6 myotubes, *FEBS Open Bio.*, 2014, **4**, 898-904.
- 462 9. T. Hatanaka, K. Kawakami and M. Uraji, Inhibitory effect of collagen-derived  
463 tripeptides on dipeptidylpeptidase-IV activity, *J. Enzyme Inhib. Med. Chem.*,  
464 2014, **29**, 823-828.
- 465 10. I. M. Lacroix and E. C. Li-Chan, Comparison of the susceptibility of porcine and  
466 human dipeptidyl-peptidase IV to inhibition by protein-derived peptides,  
467 *Peptides*, 2015, **69**, 19-25.

- 468 11. C. C. Udenigwe and R. E. Aluko, Food protein-derived bioactive peptides  
469 production, processing, and potential health benefits, *J. Food Sci.*, 2012, **77**,  
470 R11-R24.
- 471 12. E. C. Y. Li-Chan, Bioactive peptides and protein hydrolysates: research trends  
472 and challenges for application as nutraceuticals and functional food ingredients,  
473 *Curr. Opin. Food Sci.*, 2015, **1**, 28-37.
- 474 13. S. C. de C. Zani, J. Wu and C. B. Chan, Egg and soy-derived peptides and  
475 hydrolysates: a review of their physiological actions against diabetes and  
476 obesity, *Nutrients*, 2018, **10**, 5, 549.
- 477 14. A. C. Neves, P. A. Harnedy, M. B. O'Keeffe and R. J. FitzGerald, Bioactive  
478 peptides from Atlantic salmon (*Salmo salar*) with angiotensin converting  
479 enzyme and dipeptidyl peptidase IV inhibitory, and antioxidant activities, *Food*  
480 *Chem.*, 2017, **218**, 396-405.
- 481 15. P. A. Harnedy, M. B. O'Keeffe and R. J. FitzGerald, Purification and  
482 identification of dipeptidyl peptidase (DPP) IV inhibitory peptides from the  
483 macroalga *Palmaria palmata*, *Food Chem.*, 2015, **172**, 400-406.

- 484 16. P. Patil, S. Mandal, S. K. Tomar and S. Anand, Food protein-derived bioactive  
485 peptides in management of type 2 diabetes, *Eur. J. Nutr.*, 2015, **54**, 863-880.
- 486 17. R. de C. L. Lima, K. T. Kongstad, L. Kato, M. J. Silva, H. Franzyk and D. Staerk,  
487 High-resolution PTP1B inhibition profiling combined with HPLC-HRMS-SPE-  
488 NMR for identification of PTP1B inhibitors from *Miconia albicans*, *Molecules*,  
489 2018, **23**, 1755.
- 490 18. K. T. Kongstad, S. G. Wubshet, L. Kjellerup, A. M. L. Winther and D. Staerk,  
491 Fungal plasma membrane H(+)-ATPase inhibitory activity of *o*-  
492 hydroxybenzylated flavanones and chalcones from *Uvaria chamae* P. Beauv.,  
493 *Fitoterapia*, 2015, **105**, 102-106.
- 494 19. Y. Tahtah, K. T. Kongstad, S. G. Wubshet, N. T. Nyberg, L. H. Jonsson, A. K.  
495 Jager, S. Qinglei and D. Staerk, Triple aldose reductase/alpha-  
496 glucosidase/radical scavenging high-resolution profiling combined with high-  
497 performance liquid chromatography-high-resolution mass spectrometry-solid-  
498 phase extraction-nuclear magnetic resonance spectroscopy for identification of



- 499 antidiabetic constituents in crude extract of *Radix scutellariae*, *J. Chromatogr.*  
500 *A*, 2015, **1408**, 125-132.
- 501 20. S. G. Wubshet, N. T. Nyberg, M. V. Tejesvi, A. M. Pirtila, M. Kajula, S. Mattila  
502 and D. Staerk, Targeting high-performance liquid chromatography-high-  
503 resolution mass spectrometry-solid-phase extraction-nuclear magnetic  
504 resonance analysis with high-resolution radical scavenging profiles - Bioactive  
505 secondary metabolites from the endophytic fungus *Penicillium namyslowskii*, *J.*  
506 *Chromatogr. A*, 2013, **1302**, 34-39.
- 507 21. S. G. Wubshet, I. Måge, U. Böcker, D. Lindberg, S. H. Knutsen, A. Rieder, D.  
508 A. Rodriguez and N. K. Afseth, FTIR as a rapid tool for monitoring molecular  
509 weight distribution during enzymatic protein hydrolysis of food processing by-  
510 products, *Anal. Methods*, 2017, **9**, 4247-4254.
- 511 22. I. M. Al-masri, M. K. Mohammad and M. O. Tahaa, Inhibition of dipeptidyl  
512 peptidase IV (DPP IV) is one of the mechanisms explaining the hypoglycemic  
513 effect of berberine, *J. Enzyme Inhib. Med. Chem.*, 2009, **24**, 1061-1066.

- 514 23. S. B. Rønning, M. E. Pedersen, P. V. Andersen and K. Holm, View Article Online  
https://doi.org/10.1039/C9FO02450B The  
515 combination of glycosaminoglycans and fibrous proteins improves cell  
516 proliferation and early differentiation of bovine primary skeletal muscle cells,  
517 *Differentiation*, 2013, **86**, 13-22.
- 518 24. J. Cox and M. Mann, MaxQuant enables high peptide identification rates,  
519 individualized p.p.b.-range mass accuracies and proteome-wide protein  
520 quantification, *Nat. Biotechnol.*, 2008, **26**, 1367-1372.
- 521 25. O. Power, A. B. Nongonierma, P. Jakeman and R. J. FitzGerald, Food protein  
522 hydrolysates as a source of dipeptidyl peptidase IV inhibitory peptides for the  
523 management of type 2 diabetes, *Proc. Nutr. Soc.*, 2014, **73**, 34-46.
- 524 26. A. B. Nongonierma and R. J. FitzGerald, Dipeptidyl peptidase IV inhibitory and  
525 antioxidative properties of milk protein-derived dipeptides and hydrolysates,  
526 *Peptides*, 2013, **39**, 157-163.
- 527 27. R. M. Witteles, K. V. Keu, A. Quon, H. Tavana and M. B. Fowler, Dipeptidyl  
528 peptidase 4 inhibition increases myocardial glucose uptake in nonischemic  
529 cardiomyopathy, *J. Card. Fail.*, 2012, **18**, 804-809.

*Manuscript for Food & Function*

- 530 28. A. Doyen, C. C. Udenigwe, P. L. Mitchell, A. Marette, R. E. Aluko and L. Bazinet, View Article Online  
DOI: 10.1039/C3FO002450B
- 531 Anti-diabetic and antihypertensive activities of two flaxseed protein hydrolysate
- 532 fractions revealed following their simultaneous separation by electrodialysis with
- 533 ultrafiltration membranes, *Food Chem.*, 2014, **145**, 66-76.
- 534 29. C. Roblet, A. Doyen, J. Amiot, G. Pilon, A. Marette and L. Bazinet, Enhancement
- 535 of glucose uptake in muscular cell by soybean charged peptides isolated by
- 536 electrodialysis with ultrafiltration membranes (EDUF): activation of the AMPK
- 537 pathway, *Food Chem.*, 2014, **147**, 124-130.
- 538 30. B. Viollet and F. Andreelli, AMP-activated protein kinase and metabolic control,
- 539 *Handb. Exp. Pharmacol.*, 2011, **203**, 303-330.
- 540 31. K. A. Coughlan, R. J. Valentine, N. B. Ruderman, A. K. Saha, AMPK activation:
- 541 a therapeutic target for type 2 diabetes?, *Diabetes Metab. Syndr. Obes.*, 2014,
- 542 **7**, 241-253.
- 543 32. N. G. Musi and L. J. Goodyear, AMP-activated protein kinase and muscle
- 544 glucose uptake, *Acta Physiol. Scand.*, 2003, **178**, 337-345.

- 545 33. D. G. Hardie, AMP-activated protein kinase - an energy sensor that regulates  
546 all aspects of cell function, *Genes Dev.*, 2011, **25**, 1895-1908.
- 547 34. T. L. Merry and G. K. McConell, Skeletal muscle glucose uptake during  
548 exercise: a focus on reactive oxygen species and nitric oxide signaling, *IUBMB*  
549 *Life*, 2009, **61**, 479-484.
- 550 35. R. de C. L. Lima, S. M. Gramsbergen, J. Van Staden, A. K. Jager, K. T.  
551 Kongstad and D. Staerk, Advancing HPLC-PDA-HRMS-SPE-NMR analysis of  
552 coumarins in *Coleonema album* by use of orthogonal reversed-phase C18 and  
553 pentafluorophenyl separations, *J. Nat. Prod.*, 2017, **80**, 1020-1027.
- 554 36. The human metabolome database,  
555 [http://www.hmdb.ca/spectra/ms\\_ms/296333#references](http://www.hmdb.ca/spectra/ms_ms/296333#references) (accessed November  
556 2018).
- 557 37. R. Tudela, A. Ribas-Agustí, S. Buxaderas, M. Riu-Aumatell, M. Castellari and  
558 E. López-Tamames, Ultrahigh-performance liquid chromatography (UHPLC)-  
559 tandem mass spectrometry (MS/MS) quantification of nine target indoles in  
560 sparkling wines, *J. Agric. Food Chem.*, 2016, **64**, 4772-4776.

561 38. MoNA Mass bank of North America View Article Online  
DOI: 10.1039/C9FO02450B

562 [http://mona.fiehnlab.ucdavis.edu/spectra/display/HMDB0000706\\_ms\\_ms\\_989](http://mona.fiehnlab.ucdavis.edu/spectra/display/HMDB0000706_ms_ms_989)

563 (accessed November 2018).

564 39. The Human metabolome database,

565 [http://www.hmdb.ca/spectra/ms\\_ms/294085#conditions](http://www.hmdb.ca/spectra/ms_ms/294085#conditions) (accessed November

566 2018).

567 40. V. T. T. Lan, I. Keisuke, M. Ohno, T. Motoyama, S. Ito and Y. Kawarasaki,

568 Analyzing a dipeptide library to identify human dipeptidyl peptidase IV inhibitor,

569 *Food Chem.*, 2015, **175**, 66-73.

570 41. A. Connolly, M. B. O'Keeffe, A. B. Nongonierma, C. O. Piggott and R. J.

571 FitzGerald, Isolation of peptides from a novel brewers spent grain protein isolate

572 with potential to modulate glycaemic response, *Int. J. Food Sci. & Technol.*,

573 2017, **52**, 146-153.

574 42. Alice B. Nongonierma, C. Mooney, D. C. Shields and R. J. FitzGerald, Inhibition

575 of dipeptidyl peptidase IV and xanthine oxidase by amino acids and dipeptides,

576 *Food Chem.*, 2013, **141**, 644-653.

- 577 43. A. S. Noguerola, B. Murugaverl and K. J. Voorhees, An investigation of View Article Online  
DOI: 10.1039/C9FO02450B
- 578 dipeptides containing polar and non-polar side groups by Curie-point pyrolysis
- 579 tandem mass spectrometry, *J. Am. Soc. Mass Spectrom.*, 1992, **3**, 750-756.
- 580 44. D. R. Magnin, J. A. Robl, R. B. Sulsky, D. J. Augeri, Y. Huang, L. M. Simpkins,
- 581 P. C. Taunk, D. A. Betebenner, J. G. Robertson, B. E. Abboa-Offei, A. Wang,
- 582 M. Cap, L. Xin, L. Tao, D. F. Stikoff, M. F. Malley, J. Z. Gougoutas, A. Khanna,
- 583 Q. Huang, S. P. Han, R. A. Parker and L. G. Hamann, Synthesis of novel potent
- 584 dipeptidyl peptidase IV inhibitors with enhanced chemical stability: interplay
- 585 between the N-terminal amino acid alkyl side chain and the cyclopropyl group
- 586 of  $\alpha$ -aminoacyl-L-*cis*-4,5-methanoprolinenitrile-based inhibitors, *J. Med. Chem.*,
- 587 2004, **47**, 2587-2598.
- 588 45. A. B. Nongonierma, C. Mooney, D. C. Shields and R. J. FitzGerald, *In silico*
- 589 approaches to predict the potential of milk protein-derived peptides as dipeptidyl
- 590 peptidase IV (DPP-IV) inhibitors, *Peptides*, 2014, **57**, 43-51.
- 591 46. M. Engel, T. Hoffmann, L. Wagner, M. Wermann, U. Heiser, R. Kiefersauer, R.
- 592 Huber, W. Bode, H.-U. Demuth and H. Brandstetter, The crystal structure of

593 dipeptidyl peptidase IV (CD26) reveals its functional regulation and enzymatic

View Article Online  
DOI: 10.1039/C9FO02450B

594 mechanism, *PNAS*, 2003, **100**, 5063-5068.

595

596

597

598

599

600

601

## 602 **Figure captions**

603 **Figure 1.** Schematic representation of the analysis of protein hydrolysates from mechanical  
604 chicken deboning residue. Enzymatic hydrolysis experiments were performed to afford four  
605 different hydrolysates (RC80, RC240, RF80 and RF240) and after preliminary screening for  
606 DPP-IV inhibitory activity, RC80 was selected for SEC fractionation. The SEC fractionation  
607 afforded eight fractions, which were evaluated for both DPP-IV inhibitory activity and glucose  
608 uptake. Fraction F5 was further fractionated using reversed-phase chromatography, and all  
609 fractions were assessed for DPP-IV inhibitory activity. The five most potent fractions were  
610 analyzed using LC-HRMS/MS for identification of the peptides in the fractions.

611

612 **Figure 2.** Size exclusion chromatographic trace (at 214 nm) of RC80 (**A**) and semi-high  
613 resolution DPP-IV inhibition profile of the corresponding fractions (**B**). The DPP-IV inhibition  
614 measurements were performed in triplicate and average of the three measurements is shown

615 with standard deviation. Plotted in red together with the chromatographic trace is retention time  
616 of the molecular weight standards.

617

618 **Figure 3.** Effect of the SEC fractions (F1-F8) on cellular glucose uptake and metabolic active  
619 cells. Bar plot of the relative amount of glucose uptake in cells treated with hydrolysate fractions  
620 compared to control cells (i.e., cells without addition of 2DG (-2D), cells treated with stop  
621 buffer before addition of 2DG (stopped), untreated cells, cells treated with 1 mM insulin) (A).  
622 Bar plot of the amount of ATP present in cells treated with hydrolysate fractions compared to  
623 untreated control cells (B). The data is presented as the average of at least two independent cell  
624 culture experiments seeded out in triplicates  $\pm$ SEM.

625

626 **Figure 4.** Reversed-phase chromatographic trace (at 214 nm) of F5 (A) and semi-high  
627 resolution DPP-IV inhibition profile of the corresponding fractions (B). The DPP-IV inhibition  
628 was performed in triplicate and average of the three measurements is shown with standard  
629 deviation. Five fractions with DPP-IV inhibition greater than 80% were selected for further  
630 analysis and are highlighted in red. Fractions with only duplicate measurements are presented  
631 as an average value without standard deviation (marked with '\*').

632

633 **Figure 5.** Base peak chromatograms of the five fractions F5-4 (A), F5-5 (B), F5-13 (C), F5-14  
634 (D) and F5-16 (E).

635

636 **Figure 6.** Example of HRMS spectra obtained from LC-HRMS/MS analyses of the peptides  
637 from fraction F5-13. LC-HRMS/MS spectrum of the molecular ion  $m/z$  318.1667 from the



638 peptide eluted as peak 7 (**A**) and the molecular ion  $m/z$  461.2240 from the peptide eluted as  
 639 peak 8 (**B**). After identification of characteristic fragment ions, the peptide eluted as peak 7 and  
 640 8 were identified as LAD and VEVD, respectively. Inserted to the top right are structures of the  
 641 peptides with ion fragments identified in the spectrum.

642

643

644

645

646

## 647 **Tables**

648 **Table 1.** Screening of DPP-IV activity of mechanical chicken deboning residues hydrolysates.

<b>Samples</b>	<b>1000 <math>\mu\text{g/mL}</math></b>	<b>SD</b>	<b>10 <math>\mu\text{g/mL}</math></b>	<b>SD</b>
<b>RC80</b>	59.87	0.634	20.44	1.341
<b>RC240</b>	49.82	1.692	20.61	0.975
<b>RF80</b>	51.62	7.766	21.50	0.518
<b>RF240</b>	45.94	7.518	21.24	0.701

649  $n = 3$ ; SD: Standard Deviation

650

651

652

653

654

655

656

657 **Table 2.** LC-MS/MS data of identification of peptides in the DPP-IV inhibiting RP fractions. Retention time, MS and MS/MS data is presented  
658 with the sequence of the identified peptides.

Peak	Retention time (min.)	m/z [M+H] <sup>n+</sup> (MF, ppm)	Diagnostic fragment ions (MS/MS)	Peptides
1a	8.6	233.1499 [M+H] <sup>+</sup> (C <sub>10</sub> H <sub>21</sub> N <sub>2</sub> O <sub>4</sub> <sup>+</sup> , Δ 1.4 ppm)	86.0960; 120.0670	TL
2 <sup>†</sup>	9.0	476.2308 [M+H] <sup>+</sup> (C <sub>10</sub> H <sub>21</sub> N <sub>2</sub> O <sub>4</sub> <sup>+</sup> , Δ 1.4 ppm)	-	-
3	9.4	221.0937 [M+H] <sup>+</sup> (C <sub>11</sub> H <sub>13</sub> N <sub>2</sub> O <sub>3</sub> <sup>+</sup> , Δ 7.4 ppm)	104.0538; 133.0325; 150.0595; 173.0939	5-Hydroxytryptophan (5-HT)
4	15.4	181.1128 [M+H] <sup>+</sup> (C <sub>13</sub> H <sub>17</sub> N <sub>2</sub> O <sub>5</sub> <sup>+</sup> , Δ 1.3 ppm)	120.0821	DF
5a	8.9	233.1496 [M+H] <sup>+</sup> (C <sub>10</sub> H <sub>21</sub> N <sub>2</sub> O <sub>4</sub> <sup>+</sup> , Δ 5.0 ppm)	86.0968; 120.0668	TL
6	9.5	203.1390 [M+H] <sup>+</sup> (C <sub>9</sub> H <sub>19</sub> N <sub>2</sub> O <sub>3</sub> <sup>+</sup> , Δ 4.9 ppm)	86.0968; 157.1316	LA
7	11.4	318.1667 [M+H] <sup>+</sup> (C <sub>13</sub> H <sub>24</sub> N <sub>3</sub> O <sub>6</sub> <sup>+</sup> , Δ 2.2 ppm)	86.0968; 157.1346; 185.1298; 205.0834	LAD
8	18.9	461.2242 [M+H] <sup>+</sup> (C <sub>19</sub> H <sub>33</sub> N <sub>4</sub> O <sub>9</sub> <sup>+</sup> , Δ 1.2 ppm)	134.0459; 233.1136; 362.1538	VEVD
9b	20.8	245.1860 [M+H] <sup>+</sup> (C <sub>12</sub> H <sub>25</sub> N <sub>2</sub> O <sub>3</sub> <sup>+</sup> , Δ 3.2 ppm)	86.0974; 132.1038	LL
10b	21.2	245.1877 [M+H] <sup>+</sup> (C <sub>12</sub> H <sub>25</sub> N <sub>2</sub> O <sub>3</sub> <sup>+</sup> , Δ 7.2 ppm)	86.0975; 132.1041	LL
11 <sup>†</sup>	19.2	519.6880 [M+2H] <sup>2+</sup>	-	-
12 <sup>‡</sup>	20.3	461.2318 [M+2H] <sup>2+</sup>	-	ETGKGEDGE
13 <sup>†</sup>	20.6	779.7376 [M+3H] <sup>3+</sup>	-	-
14b	21.2	245.1860 [M+H] <sup>+</sup> (C <sub>12</sub> H <sub>25</sub> N <sub>2</sub> O <sub>3</sub> <sup>+</sup> , Δ 7.0 ppm)	86.0970; 132.1032	LL
15	21.7	279.1710 [M+H] <sup>+</sup> (C <sub>15</sub> H <sub>23</sub> N <sub>2</sub> O <sub>3</sub> <sup>+</sup> , Δ 2.6 ppm)	86.0947; 120.0823; 132.1036	FL
16 <sup>†</sup>	19.2	433.7220 [M+H] <sup>6+</sup>	-	-
17 <sup>‡</sup>	20.1	382.9011 [M+H] <sup>3+</sup>	-	LFFSMLLML
18 <sup>†</sup>	20.9	474.9056 [M+3H] <sup>3+</sup>	-	-
19	21.9	279.1706 [M+H] <sup>+</sup> (C <sub>15</sub> H <sub>23</sub> N <sub>2</sub> O <sub>3</sub> <sup>+</sup> , Δ 0.9 ppm)	86.0947; 120.0823; 166.0875	LF

659 All peptides identified with leucine residue (L) can interchangeably be the isobaric isoleucine (I)

660 <sup>a,b</sup>Peptides identified in more than one fraction.

661 <sup>†</sup>Unidentified peptides.

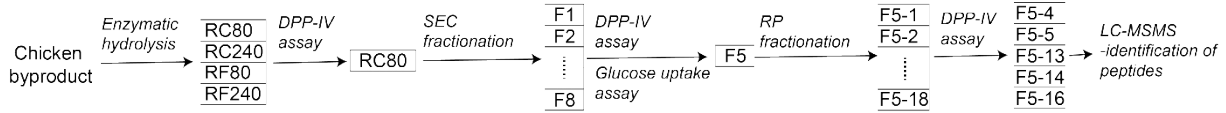
662 <sup>‡</sup>Peptides identified using MaxQuant<sup>24</sup>.

663 **Figures**

View Article Online  
DOI: 10.1039/C8FO02450B

664 **Figure 1.**

665

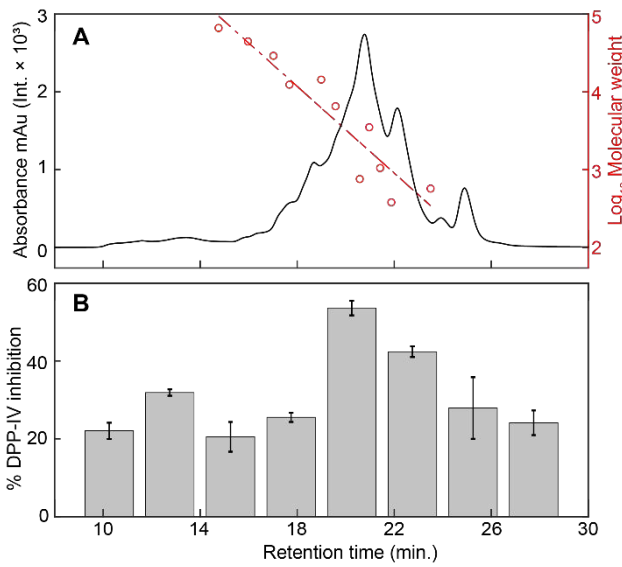


666

667

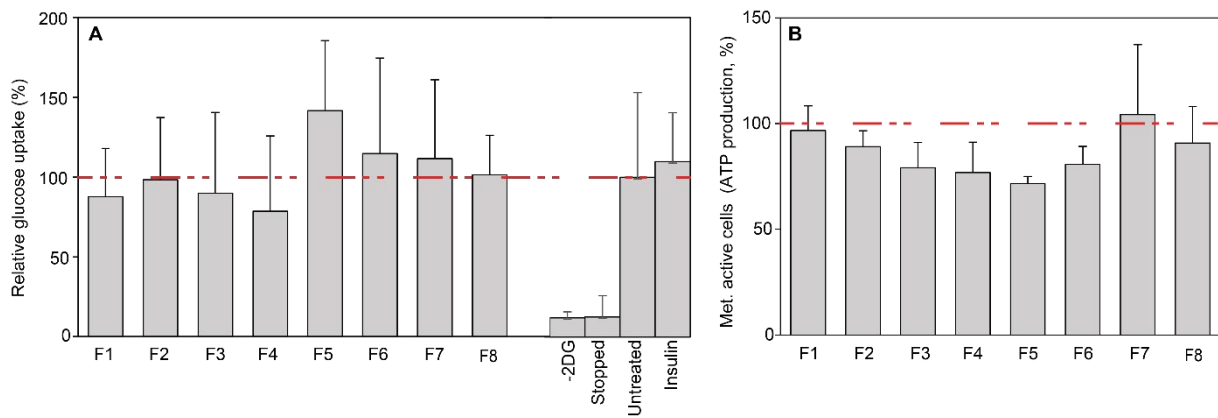
668

669 **Figure 2.**



670

671 **Figure 3.**



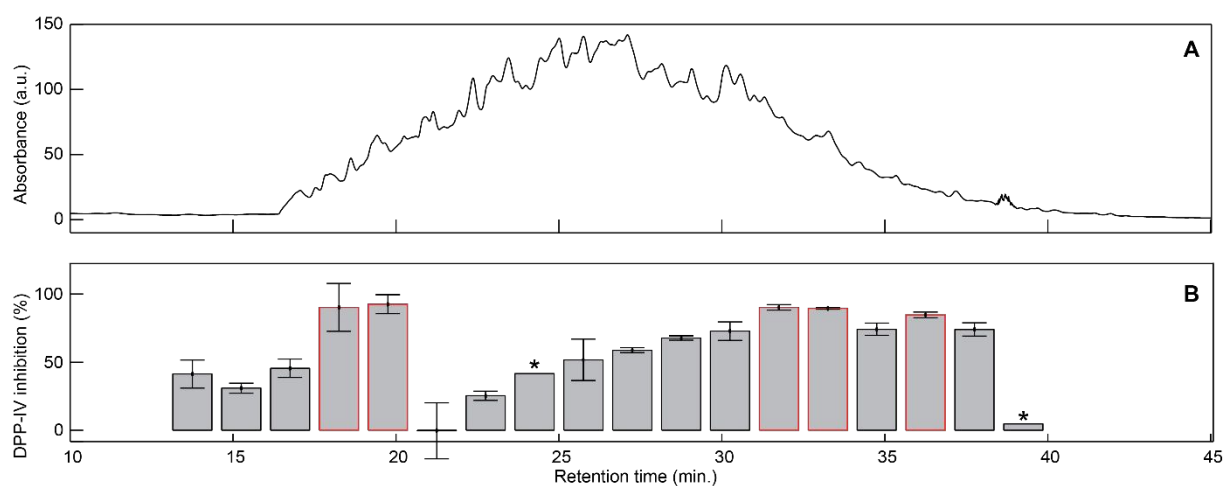
672

673

674

675

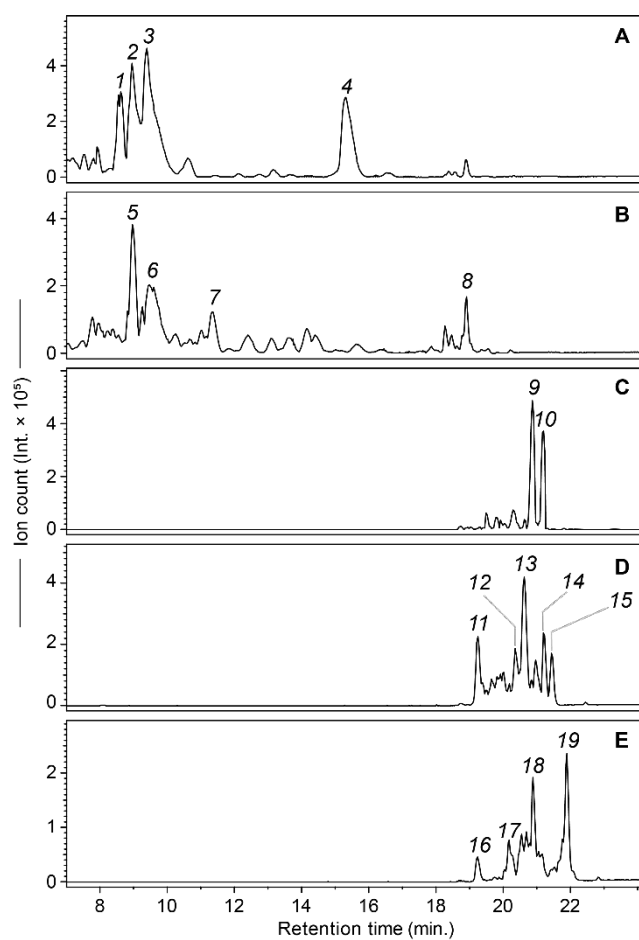
676

677 **Figure 4.**View Article Online  
DOI: 10.1039/C8FO02450B

678

679

680

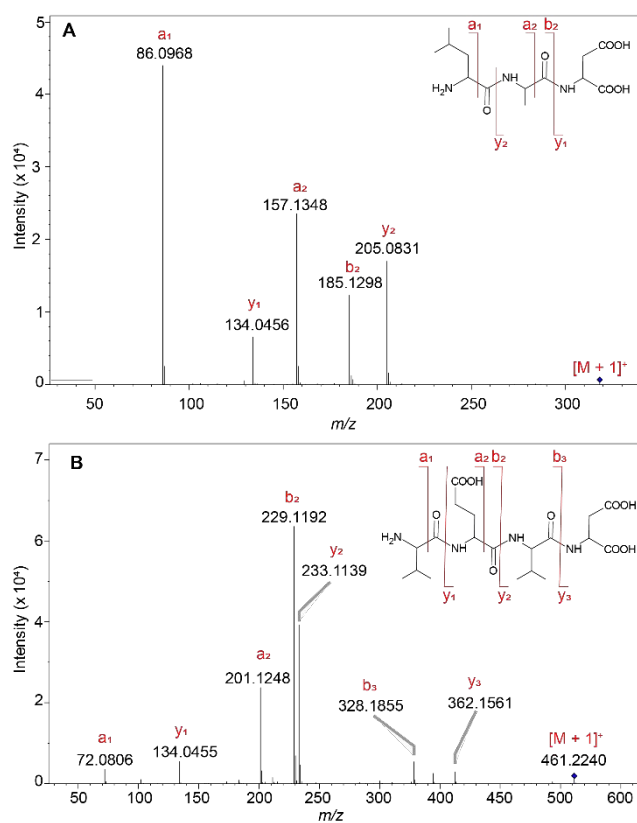
681 **Figure 5**

682

683

684

685

686 **Figure 6.**View Article Online  
DOI: 10.1039/C8FO02450B

687

688

689

690

691

692

693

694

695

696

697

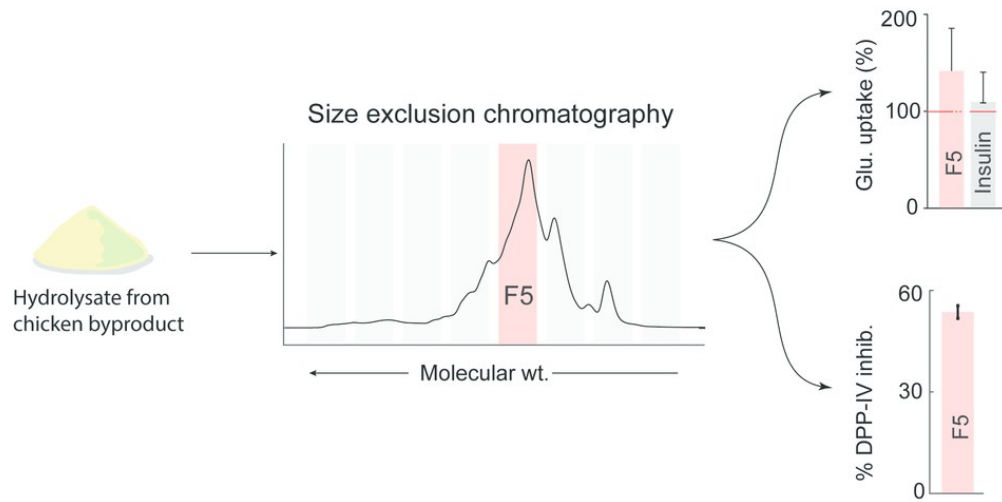
698

699

700

701

702



80x40mm (300 x 300 DPI)